MITIGATION OF SPARSELY SAMPLED NONSTATIONARY JAMMERS FOR MULTI-ANTENNA GNSS RECEIVERS

Yimin D. Zhang [†], *Moeness G. Amin* [‡], *and Ben Wang* [†♯]

[†] Department of Electrical and Computer Engineering, Temple University, Philadelphia, PA 19122, USA
[‡] Center for Advanced Communications, Villanova University, Villanova, PA 19085, USA
[♯] College of Automation, Harbin Engineering University, Harbin, Heilongjiang 150001, China

ABSTRACT

In this paper, we address the suppression of frequency modulated jammers in a multi-sensor Global Navigation Satellite System (GNSS) receiver. In particular, we consider the case of sparsely sampled signals and compressed observations. In this case, applying conventional time-frequency (TF) analysis for jammer characterization produces noise-like artifacts which, if not properly considered, would obscure the jammer TF representation and lead to considerable errors in jammer signal estimation and excision. In the proposed approach, a multi-sensor data-dependent TF kernel is applied for effective mitigation of artifacts due to missing samples. Sparse reconstruction methods are then applied to obtain nonparametric instantaneous frequency estimation. We apply the continuous-structure aware Bayesian compressive sensing method to exploit the contiguous nature of the jammer TF signature, leading to enhanced localization and suppression.

Index Terms— Navigation, anti-jamming receiver, time-frequency analysis, Bayesian compressive sensing

1. INTRODUCTION

A Global Navigation Satellite System (GNSS), such as the Global Positioning System (GPS), is vulnerable to jamming signals. As such, anti-jam capability has become essential for reliable satellite navigation. Commonly used jammers are frequency modulated (FM) signals whose level of complexity ranges from a chirp-like waveforms to higher-order polynomial phase signals. FM jammers cannot be simply mitigated by windowing or filtering. It is rather more effective to represent the jammer signals in the joint time-frequency (TF) domain where they, due to their instantaneous power concentrations, are revealed when accompanied by low power GNSS signals that are spread over the entire domain [1].

Accurate estimation of the jammer instantaneous frequencies (IFs) allows effective jammer suppression. Several techniques can be used for this purpose, including jammer waveform synthesis, time-varying notch filtering, and orthogonal projection. These techniques begin with TF signal representation where the local properties of the jammer can be captured [2, 3]. A number of methods have also been developed for parametric estimations of FM jammer signals in which the jammer polynomial phase characteristics are utilized [4–7]. It is noted that, irrespective of the employed suppression method, the use of spatial degrees of freedom through multi-antenna receiver configuration has led to a more effective IF estimation, jammer suppression and GNSS signal preservation [8–10]. Traditional anti-jamming GNSS receivers assume the jammed GNSS signals to be uniformly sampled. In real-world operations, however, samples of the jammed GNSS signals may be randomly missing due to, for example, multipath fading, line-of-sight obstructions, removal of narrow interference or impulsive noise [11]. As a result, the observed data may be sparsely sampled. Missing samples generate noise-link artifacts in the TF domain representations, making conventional approaches for anti-jam infeasible.

Recovery and/or IF estimation of FM signals from sparsely sampled observations fall under the emerging area of compressive sensing and sparse reconstruction [12–14]. Owing to their instantaneous narrowband characteristics, these signals exhibit local sparsity when viewed through a short window or when they, in general, are represented in the joint-variable TF domain. The sparsity property invites compressive sensing and sparse reconstruction techniques to play a role in anti-jam GNSS. In [12], the effect of missing samples on bilinear time-frequency distributions (TFDs) is analyzed. IF estimation based on applying a signal-dependent adaptive optimal kernel (AOK) together with sparse signal reconstruction is described. In [13], a structure-aware Bayesian compressive sensing (SA-BCS) algorithm is developed which exploits the continuous IF structure of FM signals.

We perform anti-jam for multi-antenna GNSS receivers under compressed observations [15]. In this paper, we consider the case of multiple jammers and exploit SA-BCS to estimate the IFs of the jammer signals. To account for practical multipath propagation environments, each FM jammer is assumed to have an arbitrary spatial signature, which is estimated for effective joint space-time domain jammer suppression. We use the linear model relating the TF signal representation and the instantaneous autocorrelation function (IAF) [12, 13]. The IAF in the model is generated by applying AOK so as to eliminate, or at least significantly reduce, the artifacts due to missing samples as well as cross-terms due to interactions of jammer signal components.

Notations: We use lower-case (upper-case) bold charac-

ters to denote vectors (matrices). In particular, $\mathbf{I}_N$ denotes the $N \times N$ identity matrix. $(.)^*$ denotes complex conjugation, and $(\cdot)^T$ and $(\cdot)^H$, respectively, stand for transpose and Hermitian operations. $\mathbf{F}_x$ and $\mathbf{F}_x^{-1}$ respectively denote discrete Fourier transform (DFT) and inverse DFT (IDFT) matrices with resect to x. In addition, we use $\delta(x)$ to denote the Dirac delta function of x, $\bigotimes$ the Kronecker product, and $\jmath = \sqrt{-1}$.

2. SIGNAL MODEL

GNSS signals and the associated jammers adhere to the narrowband signal model. Considering an N-elements array that receives GNSS signals $s_i(t), i = 1, \cdots, Q_S$, contaminated by FM jammer signals $s_j(t), j = 1, \cdots, Q_J$, the discrete-time received signal vector can be expressed as

$$\mathbf{y}(t) = \sum_{i=1}^{Q_S} \mathbf{h}_i s_i(t) + \sum_{j=1}^{Q_J} \mathbf{h}_j s_j(t) + \mathbf{n}(t), \tag{1}$$

for $0 \leq t \leq T-1$, where $\mathbf{h}_i$ and $\mathbf{h}_j$ are the $N \times 1$ spatial signature vectors respectively for the ith GNSS signal and the jth jammer. The jammer signals $s_j(t), j = 1, \cdots, Q_J$, are considered FM signals with a unit power. In addition, $\mathbf{n}(t)$ is the $N \times 1$ additive white Gaussian noise vector $\mathcal{CN}(0, \sigma^2 \mathbf{I}_N)$. Note that t is discretized with a sampling interval of Δt. The GNSS signals and the jammers are not required to assume a clear steering vector, making this model more practical in environment with rich multipath propagation.

Consider sparse sampling of the array observations with a random pattern applied to each array sensor. As such, for the nth array sensor, the sparse observation is given as

$$x_n(t) = y_n(t) \cdot b_n(t), \tag{2}$$

where $y_n(t)$ is the nth element of $\mathbf{y}(t)$, and $b_n(t) \in \{0, 1\}$ is the observation mask. We denote the index set of nonzero elements of $b_n(t)$ as $\mathcal{S}_n$ with cardinality $|\mathcal{S}_n| = T - M_n$. The sparsity pattern $b_n(t)$ may or may not the same for different antenna sensors.

3. TIME-FREQUENCY REPRESENTATIONS AND SPARSE RECONSTRUCTION

3.1. Adaptive Optimal Kernel

The ambiguity function (AF) for signal $x_n(t)$ is defined as [16, 17]:

$$A_n(\theta, \tau) = \int_{-\infty}^{\infty} x_n\left(t + \frac{\tau}{2}\right) x_n^*\left(t - \frac{\tau}{2}\right) e^{-\jmath 2\pi\theta t} dt, \tag{3}$$

where θ and τ are, respectively, the frequency shift (Doppler) and the time lag.

The two-dimensional (2-D) DFT of the AF is the Wigner-Ville distribution (WVD), which is usually considered as the prototype TFD before a TF kernel is applied. The WVD provides a high resolution for linear frequency modulated (LFM) signals, but it generally suffers from cross-terms when the signals are not simple LFM waveforms or contain multiple signal components.

To reduce the effect of cross-terms, which lie away from the origin in the ambiguity domain, a TF kernel function of low-pass filter characteristics is often applied to the AF. TF kernels can be data-independent or data-dependent. The latter usually yields better performance due to its adaptivity to the signal. A well-known data-dependent kernel is the AOK, which is obtained by solving the following optimization problem for AF $A(r, \psi)$ defined in the polar coordinates [18]:

$$\begin{aligned} &\max_{\Phi} \int_0^{2\pi} \int_0^{\infty} |A(r,\psi)\Phi(r,\psi)|^2 \, r dr d\psi \\ &\text{subject to} \quad \Phi(r,\psi) = \exp\left(-\frac{r^2}{2\sigma(\psi)}\right), \\ &\qquad \frac{1}{4\pi^2} \int_0^{2\pi} \sigma(\psi) d\psi \leq \alpha, \end{aligned} \tag{4}$$

where $\alpha \geq 0$ is a constant.

In a multi-sensor array platform, it is possible to design the AOK independently for each antenna. However, it is important to note that proper fusion of the multi-sensor data would produce a cleaner AF that yields a combined sensor AOK. A simple and effective strategy is to exploit the property that the AF auto-terms of the incoming signals are identical across all array sensors [9, 19] and thus can be coherently combined. We average the AFs over all sensors in (4) in lieu of only considering $A(r, \psi)$ obtained from a single sensor [20]:

$$A_\Sigma(r, \psi) = \frac{1}{N} \sum_{n=1}^{N} A_n(r, \psi). \tag{5}$$

3.2. Time-Frequency Representations through Sparse Reconstruction

In the next step, we consider the IF estimation of the jammer signals. Because the IFs are shared by all the antennas, we can compute only those corresponding to the averaged AF, $A_\Sigma(r, \psi)$. Denoted the kernelled AF in the polar coordinates as $\tilde{A}_\Sigma(r, \psi) = A_\Sigma(r, \psi)\Phi_\Sigma(r, \psi)$, which is converted to the Cartesian coordinate system as $\tilde{A}_\Sigma(\theta, \tau)$. Let $\mathbf{A}_\Sigma$ represent the AF matrix of $\tilde{A}_\Sigma(\theta, \tau)$ with all θ and τ entries.

A conventional kernelled TFD matrix is obtained by a 2-D DFT of the kernelled AF matrix, expressed as

$$\mathbf{D}_\Sigma = \mathbf{F}_\theta^{-1} \mathbf{A}_\Sigma \mathbf{F}_\tau. \tag{6}$$

Alternatively, we can obtain the TFD through sparse reconstruction from $\mathbf{A}_\Sigma$. In this case, rather than utilizing the 2-D DFT relationship between the AF and the TFD as in [19, 21], it is shown in [12, 13] that the one-dimensional (1-D) DFT relationship between the IAF and the TFD yields simpler computations and, more importantly, enables the exploitation of local sparsity in the TF domain at each time instant t.

The 1-D IDFT of $\mathbf{A}_\Sigma$ with respect to θ results in the kernelled IAF matrix $\mathbf{C}$, which is represented with respect to time t and time delay τ as

$$\mathbf{C} = \mathbf{F}_\theta^{-1} \mathbf{A}_\Sigma. \tag{7}$$

Denote $\mathbf{c}^{[t]}$ as a column of matrix $\mathbf{C}$ corresponding to time t, and $\mathbf{w}^{[t]}$ as a vector contains all the TFD entries with respect to the frequency for the same time t. Then, the 1-D DFT relationship between the IAF and the TFD becomes

$$\mathbf{c}^{[t]} = \mathbf{F}_\tau \mathbf{w}^{[t]}, \tag{8}$$

for $0 \leq t \leq T-1$. This is a standard compressive sensing formulation and can be solved by a number of methods, such as the orthogonal matching pursuit (OMP), LASSO, and Bayesian compressive sensing [22–24]. In this paper, we use the the SA-BCS algorithm [13] to perform sparse reconstruction of the TFD, which is repeated in each time instant. A brief review of the SA-BCS is provided in the following subsection. Due to the the utilization of the connected structures of the IF signature, the SA-BCS generally provides improved performance as compared to other compressive sensing methods [13, 25].

3.3. Structure-aware Bayesian compressive sensing

The SA-BCS maximizes the posterior probability of a sparse vector $\mathbf{w}^{[t]}$ given the IAF vector $\mathbf{c}^{[t]}$ as the observation. Denote $w_l^{[t]}$ as the lth element of $\mathbf{w}^{[t]}$, where $l \in [0, \ldots, T-1]$ is the frequency domain index. To encourage sparsity of the TF signatures, the following spike-and-slab prior is placed to $w_l^{[t]}$ [26], i.e.,

$$p(w_l^{[t]}|\pi_l^{[t]}, \beta_0^{[t]}) = (1-\pi_l^{[t]})\delta(w_l^{[t]}) + \pi_l^{[t]}\mathcal{CN}(w_l^{[t]}|0, [\beta_0^{[t]}]^{-1}). \tag{9}$$

Here, $\pi_l^{[t]}$ is the prior probability of a nonzero element, and $\beta_0^{[t]}$ is the precision (reciprocal of variance) of Gaussian distribution.

To make the inference analytical, we introduce the product of two latent variable $w_l^{[t]} = z_l^{[t]}\theta_l^{[t]}$ to follow the pdf in Eq. (9), where $\theta_l^{[t]}$ follows a complex Gaussian distribution $\mathcal{CN}(0, [\beta_0^{[t]}]^{-1})$ and $z_l^{[t]}$ follows the Bernoulli distribution Bern($\pi_l^{[t]}$). $z_l^{[t]}$ is a binary variable with $z_l^{[t]} = 0$ corresponding to zero value for the lth entry in the time t.

To encourage continuity pattern in the joint TF domain, we utilize data in the neighborhood time instants of $t-1$ and $t+1$, when the TF signatures in the time instant t are estimated. Based on the idea of continuity, we categorize the relationship into three different patterns. As shown in Fig. 1, different priors on $\pi_l^{[t]}$ are placed to encourage the TFD patterns with diagonal nonzero entries (Fig. 1(a)) and discourage those with all zero or all nonzero neighboring entries (Fig. 1(b)). Other patterns are placed with a neutral prior (Fig. 1(c)).

4. JAMMER SUPPRESSION THROUGH JOINT SPACE-TIME DOMAIN PROJECTION

4.1. Spatial Signature Estimation

When IFs of all the jammers are estimated as $\hat{f}_j(t), t = 1, \cdots, T$, for $j = 1, \cdots, Q_J$, the corresponding phase profile

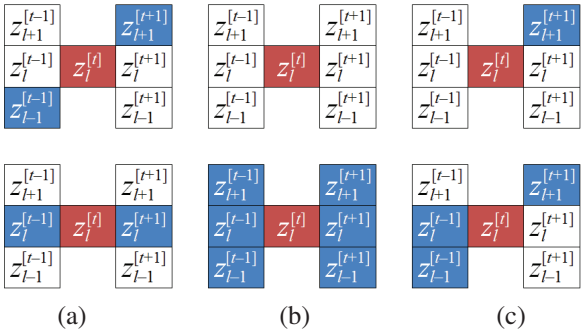

Fig. 1. Example TFD sparsity patterns. White and blue squares respectively denote zero and nonzero entries, and red squares represent the entry under test. (a) highly encouraged cases; (b) highly encouraged cases; and (c) neutral cases.

can be estimated as

$$\hat{\phi}_j(t) = 2\pi \sum_{u=0}^{t} \hat{f}_j(u)\Delta t. \tag{10}$$

The phase profile is common to all antennas up to an antenna-dependent constant phase shift for each jammer. Note that, for the actual observations, only those samples in $\mathcal{S}_n$ are available at the nth antenna. As such, we reconstruct the estimated waveform of the jth jammer at the nth antenna as

$$d_{j,n}(t) = h_{j,n} \cdot \exp(j\hat{\phi}_j(t)) \cdot b_n(t), \tag{11}$$

where $h_{j,n}$ is the nth element of $\mathbf{h}_j$ to be estimated.

For notational convenience, denote

$$d_j(t) = \exp(j\hat{\phi}_j(t)) \cdot b_n(t), \tag{12}$$

which is the sparsely sampled estimate of $s_j(t)$. When the jammer components are separable in the TF domain, the following operation yields the the maximum likelihood (ML) estimate of $a_{j,n}$

$$\hat{h}_{j,n} = \sum_{t=0}^{T-1} x_n(t) \cdot d_j^*(t) \cdot p(t), \tag{13}$$

where $p(t)$ is a window function. Here, the multiplication by $d_j^*(t)$ demodulates the received signal into the zero frequency band, commonly referred to as direct current (DC) component, and the summation amounts to low-pass filtering that accumulates the energy of the demodulated jth jammer over all T samples whereas the other jammer components and the majority of the GNSS signals are filtered out. Other TF-based filtering methods are discussed at, e.g., [27].

Note that, the estimated IFs $\hat{f}_j(t), j = 1, \cdots, Q_J$, may not be sufficiently accurate due to, for example, noise perturbation or frequency discretization error. In this case, the entire data should be partitioned into multiple segments such that the phase variation of $x_n(t) \cdot d_j^*(t)$ is insignificant over each segment. By taking the first sensor as phase reference, the spatial signatures obtained from all the segments can be coherently combined.

4.2. Jammer Suppression

We use the orthogonal projection scheme for effective jammer suppression. The received signal vector, $\tilde{\mathbf{x}} = [\mathbf{x}^T(0), \cdots, \mathbf{x}^T(T-1)]^T$, defined over the joint space-time domain, is projected into the orthogonal subspace of the estimated jammers [8]. Consider the estimated temporal signature of the jth jammer as $\hat{\mathbf{s}}_j = [d_j(0), \cdots, d_j(T-1)]^T$.The Kronecker product of the temporal signature and its spatial signature, $\mathbf{h}_j$, yields its overall subspace defined in the joint space-time domain, denoted as $\mathbf{v}_j = \hat{\mathbf{h}}_j \bigotimes \hat{\mathbf{s}}_j$, where $\hat{\mathbf{h}}_j = [\hat{h}_{j,1}, \cdots, \hat{h}_{j,N}]^T$. Let $\mathbf{V} = [\mathbf{v}_1, \cdots, \mathbf{v}_{Q_J}]$. The projection matrix into the orthogonal subspace of the jammers is given by [8]

$$\mathbf{P} = \mathbf{I}_{NT} - \mathbf{V}\left(\mathbf{V}^H\mathbf{V}\right)^{-1}\mathbf{V}^H. \tag{14}$$

The jammer-suppressed time-domain samples corresponding to the ith GNSS signal, after combining signals received at all sensors, are expressed as the following $T \times 1$ vector $\hat{\mathbf{x}}_i = \hat{\mathbf{H}}_i^H \mathbf{P}\tilde{\mathbf{x}}$,for $i = 1, \cdots, Q_S$, where $\hat{\mathbf{H}}_i = \hat{\mathbf{h}}_i \bigotimes \mathbf{I}_T$. The estimation of the spatial signature of the ith GNSS signal, $\hat{\mathbf{h}}_i$, is discussed, e.g., in [28].

5. SIMULATION RESULTS

Simulations are carried out to verify the effectiveness of the proposed method. We consider the L1 band GPS signals with the C/A codes, and a two-element (N=2) array with a half-wavelength interelement spacing is used. We set the input signal-to-noise ratio (SNR) of the GPS waveform as -16 dB. Two jammers are considered, and the input jammer-to-noise ratio (JNR) of both jammer signals are assumed to be 25 dB.

Sample the received jammed GPS signal at the chip rate of the GPS signal, which is 1.023 MHz. The normalized IF laws of the two FM jammers are assumed to be

$$f_1(t) = 0.05 + 0.05t/T + 0.1t^2/T^2, \tag{15}$$

$$f_2(t) = 0.15 + 0.05t/T + 0.1t^2/T^2, \tag{16}$$

for $t = 0, ..., T-1$, where the block size of the signal is chosen to be $T = 256$. We assume that 50% of the received data samples are randomly missing, and the missing patterns at the two antennas are uniformly and independently distributed.

We focus on one GPS signal. Due to multipath propagation, the GPS signal as well as the two jammers are assumed not to have a clear steering direction. The used spatial signatures of the GPS signal and the two jammers are represented in the following matrix:

$$\mathbf{H}=\begin{bmatrix} -1.22+0.24j & 1.39+0.66j & 0.16-0.39j \\ 1.13+0.95j & -0.44-0.35j & -0.50-0.26j \end{bmatrix}. \tag{17}$$

The magnitudes of the spatial correlation [29] between the GPS signal and the two jammers are respectively 0.625 and 0.579, whereas that between the two jammers is 0.296.

In Fig. 2(a), the real-part of the jammed GPS signal waveform received at the first antenna is shown, where the red dots represent the 64 missing data samples. The

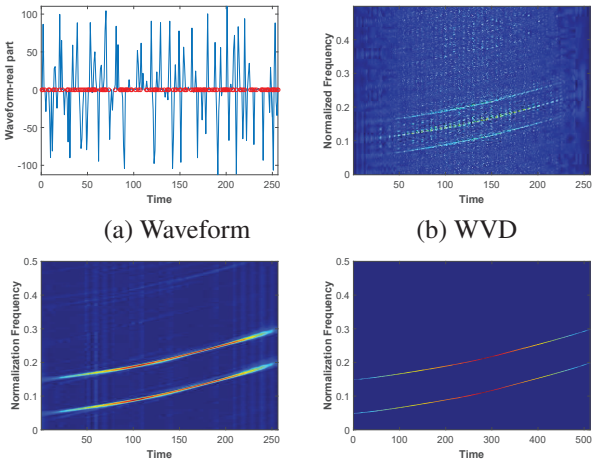

(a) Waveform (b) WVD

(c) Kernelled TFD (d) Reconstructed TFD

Fig. 2. Signal waveform and TFD results.

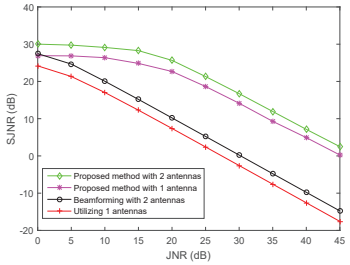

Fig. 3. Output SJNR versus input JNR.

corresponding WVD averaged over the two antennas is shown in Fig. 2(b). Due to the missing data samples, the WVD is cluttered by the artifacts which make it difficult to accurately estimate the IF of the jammer signals.

Fig. 2(c) shows the averaged TFD obtained from the 2-D DFT after applying the AOK. It is clear that the artifacts are significantly suppressed. The TFD reconstructed from the SA-BCS is shown in Fig. 2(d), which is used for estimation of the jammer IFs and the phase profiles. The entire observation period is divided into half-overlapping segments of length 32 for phase profile estimation and jammer suppression.

The yielding output SJNR, evaluated in the despread GPS symbol and averaged over the 100 independent trails, is shown in Fig. 3 where the input JNR varies between 0 dB and 45 dB. It clearly shows the effectiveness of the proposed nonstationary jammer suppression approach the improvement due to the exploitation of multiple sensors.

6. CONCLUSION

We have developed an effective FM jammer suppression method in a multi-sensor GNSS receiver suitable for compressed observations and missing samples. The proposed method first utilized the multi-sensor data-dependent kernel to mitigate the artifact. The IF estimation of the jammer signals was obtained using the recently developed SA-BCS methods. By exploiting the ML estimates of the spatial signature of each jammer, effective jammer excision is achieved through orthogonal projection in the joint space-time domain.

7. REFERENCES

[1] Y. Zhang, M. G. Amin, and A. R. Lindsey, "Anti-jamming GPS receivers based on bilinear signal distributions," in *Proc. IEEE MILCOM*, Vienna, VA, Oct. 2001, pp. 1070–1074.

[2] S. Barbarossa and A. Scaglione, "Adaptive time-varying cancellation of wideband interferences in spread-spectrum communications based on time-frequency distributions," *IEEE Trans. Signal Process.*, vol. 47, pp. 957–965, Apr. 1999.

[3] M. G. Amin and Y. Zhang,"Interference suppression in spread spectrum communication systems," in J. G. Proakis (ed.), *Wiley Encyclopedia of Telecommunications*. John Wiley, 2002.

[4] B. Boashash, "Estimating and interpreting the instantaneous frequency of a signal," *Proc. IEEE*, vol. 80, pp. 520–538, Dec. 1990.

[5] S. Barbarossa, A. Scaglione, and G. B. Giannakis, "Product high-order ambiguity function for multicomponent polynomial-phase signal modeling," *IEEE Trans. Signal Process.*, vol. 46, no. 3, pp. 691–708, 1998.

[6] C. Ioana, Y. D. Zhang, M. G. Amin, F. Ahmad, G. Frazer, and B. Himed, "Time-frequency characterization of micro-multipath signals in over-the-horizon radar," in *Proc. IEEE Radar Conf.*, Atlanta, GA, May 2012, pp. 671–675.

[7] H. Zhang, G. Bi, W. Yang, S. G. Razul, and C.-M. S. See, "IF estimation of FM signals based on time-frequency image," *IEEE Trans. Aerospace Electron. Syst.*, vol. 51, no. 1, pp. 326–343, Jan. 2015.

[8] Y. Zhang and M. G. Amin, "Array processing for nonstationary interference suppression in DS/SS communications using subspace projection tech-niques," *IEEE Trans. Signal Process.*, vol. 49, no. 12, pp. 3005–3014, Dec. 2001.

[9] W. Mu, M. G. Amin, and Y. Zhang, "Bilinear signal synthesis in array processing," *IEEE Trans. Signal Process.*, vol. 51, no. 1, pp. 90–100, Jan. 2003.

[10] Y. Zhang and M. G. Amin, "Blind separation of nonstationary sources based on spatial time-frequency distributions", *EURASIP J. Applied Signal Process.*, vol. 2006, article ID 64785, 13 pages, 2006.

[11] M. G. Amin and Y. D. Zhang, "Nonstationary jammer excision for GPS receivers using sparse reconstruction techniques," in *Proc. ION GNSS+*, Tampa, FL, Sept. 2014, pp. 3469–3474.

[12] Y. D. Zhang, M. G. Amin, and B. Himed, "Reduced interference time-frequency representations and sparse reconstruction of undersampled data," in *Proc. EUSIPCO*, Marrakech, Morocco, Sept. 2013, pp. 1–5.

[13] Q. Wu, Y. D. Zhang, and M. G. Amin, "Continuous structure based Bayesian compressive sensing for sparse reconstruction of time-frequency distribution," in *Proc. Int Conf. Digital Signal Process.*, Hong Kong, China, Aug. 2014, pp. 831–836.

[14] M. G. Amin, B. Jokanovic, Y. D. Zhang, and F. Ahmad, "A sparsity-perspective to quadratic time-frequency distributions," *Digital Signal Process.*, vol. 46, pp. 175–190, Nov. 2015.

[15] Y. D. Zhang, B. Wang, and M. G. Amin, "Multi-sensor excision of sparsely sampled nonstationary jammers for GPS receivers," in *Proc. ION GNSS+*, Tampa, FL, Sept. 2015.

[16] L. Cohen, *Time-Frequency Analysis*. Prentice Hall, 1995.

[17] B. Boashash (ed.), *Time-Frequency Signal Analysis and Processing, 2nd Edition*. Academic Press, 2015.

[18] R. G. Baraniuk and D. L. Jones, "A signal-dependent time-frequency representation: Optimal kernel design," *IEEE Trans. Signal Proc.*, vol. 41, pp. 1589–1602, April 1993.

[19] Y. D. Zhang and M. G. Amin, "Compressive sensing in nonstationary array processing using bilinear transforms," in *Proc. IEEE SAM Workshop*, Hoboken, NJ, June 2012, pp. 349–352.

[20] Y. D. Zhang, L. Guo, Q. Wu, and M. G. Amin, "Multi-sensor kernel design for time-frequency analysis of sparsely sampled non-stationary signals," in *Proc. IEEE Radar Conf.*, Arlington, VA, May 2015, pp. 896–900.

[21] P. Flandrin and P. Borgnat, "Time-frequency energy distributions meet compressed sensing," *IEEE Trans. Signal Proc.*, vol. 58, no. 6, pp. 2974-2982, 2010.

[22] J. A. Tropp and A. C. Gilbert, "Signal recovery from partial information via orthogonal matching pursuit," *IEEE Trans. Info. Theory*, vol. 53, no. 12, pp. 4655-4666, 2007.

[23] R. Tibshirani, "Regression shrinkage and selection via the Lasso," *J. Royal Statist. Soc.*, vol. 58, no. 1, pp. 267-288, 1996.

[24] S. Ji, D. Dunson, and L. Carin, "Multi-task compressive sampling," *IEEE Trans. Signal Process.*, vol. 57, no. 1, pp. 92-106, 2009.

[25] S. Qin, Y. D. Zhang, Q. Wu, and M. G. Amin, "Structure-aware Bayesian compressive sensing for near-field source localization based on sensor-angle distributions," *Int. J. Antennas Propagat.*, vol. 2015, Article ID 783467, 15 pages, March 2015.

[26] L. Yu, J. P. Barbot, G. Zheng, and H. Sun, "Compressive sensing for culster structured sparse signals: Variational Bayes approach," Tech. Rep., 2011. Available at https://hal.archives-ouvertes.fr/hal-00573953/document .

[27] H. Zhang, G. Bi, L. Zhao, S. G. Razul, and C.-M. S. See, "Time-varying filtering and separation of nonstationary FM signals in strong noise environments," in *Proc. IEEE ICASSP*, Florence, Italy, May 2014, pp. 4171–4175.

[28] Y. D. Zhang and M. G. Amin, "Anti-jamming GPS receiver with reduced phase distortions," *IEEE Signal Process. Lett.*, vol. 19, no. 10, pp. 635–638, Oct. 2012.

[29] H.-C. Lin, "Spatial correlation in adaptive arrays," *IEEE Trans. Antennas Propagat.*, vol. 30, no. 2, pp. 212–222, March 1982.